J Fluoresc (2008) 18:193–201
DOI 10.1007/s10895-007-0263-4

ORIGINAL PAPER

Oxygen-dependent Oxidation of Fe(II) to Fe(III) and Interaction of Fe(III) with Bovine Serum Albumin, Leading to a Hysteretic Effect on the Fluorescence of Bovine Serum Albumin

Xiaolong Xu · Liyun Zhang · Dengke Shen · Hao Wu · Qingliang Liu

Received: 7 June 2007 / Accepted: 24 September 2007 / Published online: 16 October 2007

Abstract The serum albumin is the most abundant protein in blood plasma and the iron is essential for many cellular processes. However, the interaction between Fe^{3+} and haem-free serum albumin remains unclear. Here we provide evidence for the fact that haem-free BSA possesses one specific Fe^{3+}-binding site. The binding of Fe^{3+} to BSA results in a significant quenching of the Trp fluorescence of BSA. The average apparent dissociation constant value for the interaction of Fe^{3+} and BSA is $3.46\times10^{-8}\pm3\times10^{-10}$ M at 37 °C and $3.30\times10^{-8}\pm5\times10^{-10}$ M at 25 °C, respectively, as determined by fluorescence titration. Addition of 50 μM Fe^{2+} to 1 μM BSA results in an obvious hysteretic effect on the fluorescence of BSA. The time-dependent fluorescence quenching of BSA by Fe^{2+} is not caused by the Fe^{2+}-induced conformational change of BSA, but the oxygen-dependent oxidation of Fe^{2+} to Fe^{3+}. Fe^{2+} undergoes an oxygen-dependent oxidation to Fe^{3+} under aerobic conditions, which is accelerated by the interaction of BSA with Fe^{3+} and extensively inhibited under anaerobic conditions. The results suggest that BSA may take part in non-transferrin bound iron transfer.

Keywords Bovine serum albumin · Iron · Fluorescence · Hysteretic effect

X. Xu (✉) · L. Zhang · D. Shen · H. Wu · Q. Liu
Department of Chemistry,
University of Science and Technology of China,
Hefei 230026, People's Republic of China
e-mail: xuxl@ustc.edu.cn

Introduction

Iron is essential for many cellular processes based on the fact that the function of numerous cellular proteins is coupled to the intramolecular presence of this transition metal [1]. The major part of the cellular iron is safely bound in ferritin as well as in haem- or iron–sulphur cluster-containing proteins (enzymes) [2–6]. A small part (0.2–3%) is loosely attached to proteins or lipids or weakly bound to low-molecular-mass ligands like phosphates, citric acid, amino acids, sugars, ascorbate, ADP, and ATP, forming a transit iron pool that keeps iron available for the synthesis of iron-containing proteins [7].

The serum albumin is the most abundant protein in blood plasma. The protein is principally characterized by its remarkable ability to bind a broad range of hydrophobic small molecule ligands including fatty acids, haem, bilirubin, thyroxine, bile acids and steroids; it serves as a solubilizer and transporter for these compounds and, in some cases, provides important buffering of the free concentration [8–12]. Serum albumin also binds a wide variety of drugs [13–17]. The protein has been also implicated in transport, storage, and metabolism of many metal ions, and have many physiological functions as the major constituents of the circulatory system [18–21]. Many studies have been carried out to characterize the binding of serum albumin with metal ions, such as Zn^{2+}, Cu^{2+}, Ni^{2+}, Co^{2+}, Cd^{2+}, Ca^{2+}, Mg^{2+} and Pb^{2+} [22–28], and the complexes of metal ions, such as iron-haem, iron-nitrilotriacetate and Fe^{3+}-pyridoxal isonicotinoyl hydrazone [29–33]. A hysteretic effect, i.e. Co^{2+} or Ni^{2+}-induced slow conformational transition of HSA or BSA, has been observed in the interaction of Co^{2+} or Ni^{2+} with HSA

or BSA [25, 34]. However, studies have rarely been carried out on the interaction between Fe^{3+} and haem-free serum albumin.

Fluorescence spectroscopy is an important analytical technique suitable for study of the conformational changes of protein due to its inherent sensitivity [35–37]. Therefore it has been used to investigate whether haem-free BSA binds with ironic ions and if the interaction causes any slow conformational transition of BSA. The results presented here indicate that BSA possesses one specific Fe^{3+}-binding site. The binding of Fe^{3+} to BSA does not cause any hysteretic effect on the fluorescence of BSA, while addition of 50 μM Fe^{2+} ions to 1 μM BSA results in an obvious hysteretic effect on the fluorescence of BSA. The time-dependent fluorescence quenching of BSA by Fe^{2+} is not caused by the Fe^{2+}-induced conformational change of BSA, but the oxygen-dependent oxidation of Fe^{2+} to Fe^{3+}, which is accelerated by the interaction of BSA with Fe^{3+}. *The results presented here provide new insights into BSA functions as a non-transferrin bound iron transfer and as an accelerator for the oxygen-dependent oxidation of* Fe^{2+} to Fe^{3+}.

Materials and methods

Materials

$FeCl_3 \cdot 6H_2O$, $FeCl_2 \cdot 4H_2O$, $MnCl_2 \cdot 4H_2O$, $CoCl_2 \cdot H_2O$, $CuCl_2 \cdot 2H_2O$, $NiCl_2 \cdot 6H_2O$, $CaCl_2$, and BSA were obtained from Sigma Chemical Company. The theoretical extinction coefficient (ε=47,790 M^{-1} cm^{-1}) derived from the sequence of BSA by the ExPASy ProtParam software was used to determine its concentration. Chelex-100 was purchased from Bio-Rad Laboratories (Richmond, Calif. USA). All other reagents were of analytical reagent grade. Milli-Q purified water was used throughout.

Solutions

The solutions of Fe^{3+}, Mn^{2+}, Co^{2+}, Cu^{2+}, Ni^{2+}, and Ca^{2+} ions were prepared from $FeCl_3 \cdot 6H_2O$, $MnCl_2 \cdot 4H_2O$, $CoCl_2 \cdot H_2O$, $CuCl_2 \cdot 2H_2O$, $NiCl_2 \cdot 6H_2O$, and $CaCl_2$ in Milli-Q water, respectively, and standardized by titration with standard EDTA solution. Fe^{2+} ion was prepared from $FeCl_2$ temporarily. One gram of iron powder was added to 50 ml of 100 mM Fe^{2+} solution to avoid the oxidation of Fe^{2+} to Fe^{3+} and the iron powder was removed from the solution by centrifugation before use. Buffers and water used in the metal-binding experiments were passed through Chelex-100 to remove extraneous metal salts.

Steady-state fluorescence measurements

All fluorescence measurements were performed on a LS55 Luminescence spectrometer (Perkin-Elmer instruments USA) using a 10 mm quartz cuvette. The sample temperature was kept at 25.0 °C with a circulating water bath. In all experiments, the samples were excited at *295 nm*, and the bandwidths for excitation and emission were both set to 5 nm. Each spectrum is the average of three consecutively acquired spectra. All spectra were corrected by subtracting the spectrum of the blank, lacking the protein but otherwise identical to the sample. For titration of BSA in 0.05 M Tris–HCl (pH 7.4) with Fe^{3+}, the solution of Fe^{3+} at an appropriate concentration was added to 1 ml of 1 μM BSA serially in small aliquots, and the fluorescence spectra were recorded after each addition with excitation at 295 nm in the spectrofluorometer. The fluorescence intensities were corrected for changes in volume.

Calculation of dissociation constant K_d

The K_d value for the binding of the Fe^{3+} to BSA was determined by fitting the fluorescence titration data to a simple bimolecular association model as described by Leonard et al. [38]. The association between BSA and Fe^{3+} can be described by the following equation

$$\mathrm{BSA} + \mathrm{Fe}^{3+} \leftrightarrow \mathrm{Fe}^{3+} - \mathrm{BSA} \tag{1}$$

The fluorescence intensity (F) is related to the dissociation constant, K_d as follows,

$$F = F_0 + (F_t - F_0)\left[\frac{(K_d + P_0 + M) - \sqrt{(K_d + P_0 + M)^2 - 4P_0M}}{2P_0}\right] \tag{2}$$

where F_0 and F_t are the fluorescence intensities at the starting and end points of the titration, respectively. P_0 is the total concentration of BSA and M is the total concentration of the Fe^{3+} at any point in the titration. Fitting of data was carried out using the computer program Microcal Origin™ 6.0 (Northampton, MA). Average K_d value was determined from three independent measurements.

Circular dichroism (CD) measurements

CD measurements were carried out with a Jasco J-810 spectropolarimeter. The instrument was calibrated with *d*-10-camphorsulphonic acid. All the CD measurements were made at 25 °C with a thermostatically controlled cell holder. Far-UV CD spectra were collected between 200 and 250 nm with a scan speed of 20 nm/min and a response

time of 1 s, at a protein concentration of 0.15 mg/ml, in quartz cells of 1 mm path length. The obtained values were normalized by subtracting the baseline recorded for the buffer having same concentration of salts under similar conditions. The data were expressed in mean residue ellipticity $[\theta]$ in deg·cm^2·dmol^{-1}, which is defined as $[\theta]=100\theta_{obs}(lc)^{-1}$, where θ_{obs} is the observed ellipticity in degrees, c is the concentration in residue moles per liter, and l is the length of the light path in centimeter.

Equilibrium dialysis

Equilibrium dialysis was performed at 4 °C in a micro-volume dialyzer with 250 μl of cells (Hoffer Scientific Instrument, San Francisco, CA) in 0.01 M Tris–HCl (pH 7.4). Dialysis membranes were pretreated with a boiled solution of 0.1 M $NaHCO_3$ and 2% EDTA, and washed extensively with Milli-Q water. A 200 μl aliquot of a solution of 50–100 μM $FeCl_3$ was dialyzed against 200 μl of a solution of BSA (25 μM) for 48 h with constant rotation. Fe^{3+} ions were determined with inductively coupled plasma atomic emission spectrometry (ICP-AES), Model Atomscan Advantage, (Thermo Jarrell Ash, USA). The moles of bound Fe^{3+} ions/mol of BSA (r) were calculated by

$$r = \left([Fe^{3+}]_1 - [Fe^{3+}]_2\right)/[BSA] \quad (3)$$

Where $[Fe^{3+}]_1$ and $[Fe^{3+}]_2$ are the concentrations of Fe^{3+} ions in the solution of BSA and the solution of $FeCl_3$, respectively, when the two solutions have reached equilibrium, and [BSA] is the concentration of BSA.

UV and fourth-derivative spectroscopy

UV and fourth-derivative spectra were taken on a UV-3700 spectrophotometer (Shimadzu, Japan), using a derivative interval of 10 nm, a slit width of 3 nm, a time constant of 1 s, and a scan rate of 100 nm/min for fourth-derivative spectra. The samples were taken at 25 °C in duplicate.

Results

Steady-state fluorescence of tryptophan

BSA has two Trp residues, Trp-135 and Trp-214. To examine the binding of metal ions to BSA and the metal ions-induced hysteretic effect on BSA, the fluorescence measurements of BSA were performed at an excitation wavelength of 295 nm at 25 °C. Upon excitation at 295 nm only the Trp residue emission is observed. The maximum emission of BSA is at 348 nm by excitation at 295 nm (data not shown). The effects of Fe^{3+}, Fe^{2+}, Mn^{2+}, Co^{2+}, Cu^{2+}, Ni^{2+} and Ca^{2+} ions on the fluorescence of BSA are displayed in Fig. 1. Addition of 50 μM Mn^{2+}, Co^{2+}, Ni^{2+} or Ca^{2+} ions to 1 μM BSA induces a slight effect on of the Trp fluorescence of BSA, and no hysteretic effect on BSA has been observed for these metal ions. Addition of 50 μM Cu^{2+} ions to 1 μM BSA induces an obvious quenching (~38%) of the Trp fluorescence of BSA with no detectable shift in the emission maximum. The fast fluorescence quenching of BSA is due to the rapid binding of Cu^{2+} to the first three amino acids of BSA [23]. Cu^{2+} also does not induce any slow conformational transition of BSA. Addition of 50 μM Fe^{3+} ions to 1 μM BSA induces a significant quenching (~76%) of the Trp fluorescence of BSA with no obvious shift in the emission maximum, which may be caused by the direct collisional quenching of the Trp fluorescence in BSA or the complex formation between the protein and Fe^{3+} ions. Addition of 50 μM Fe^{2+} ions to 1 μM BSA induces a time-dependent quenching of the Trp fluorescence of BSA. The kinetics of Fe^{2+}-induced fluorescence quenching **is** best fitted to a one-exponential term yielding quenching rate constant value of 0.131±0.001 min^{-1}. The hysteretic effect on the fluorescence of BSA may be caused by the Fe^{2+}-induced slow conformational transition of BSA or the possible oxidation of Fe^{2+} to Fe^{3+}.

Figure 2 shows the effect of Fe^{3+} on the fluorescence of free tryptophan. The fluorescence intensity of free tryptophan at 355 nm at pH 7.4 by exciting at 295 nm decreases by 15.6% upon addition of 50 μM Fe^{3+} ions. As shown in the inset figure in Fig. 2, the Fe^{3+} solution has slight UV absorption at the maximum excitation wavelength (295 nm) and the maximum emission wavelength (355 nm) of free

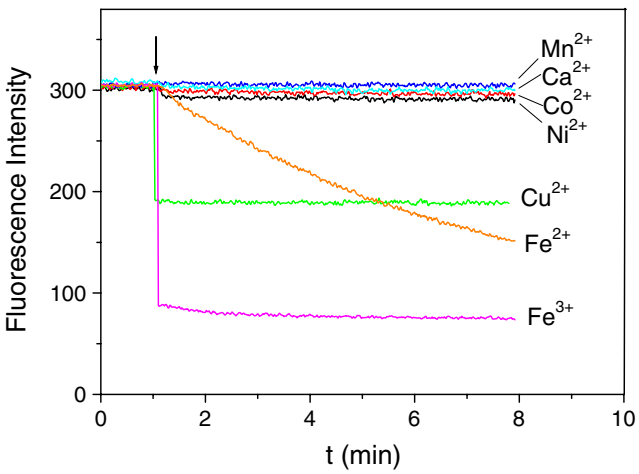

Fig. 1 The effects of Fe^{3+}, Fe^{2+}, Mn^{2+}, Co^{2+}, Cu^{2+}, Ni^{2+} and Ca^{2+} ions on the fluorescence of BSA. The fluorescence of 1 μM BSA in 0.05 M Tris–HCl (pH 7.4) was measured at 348 nm by exciting at 295 nm in time-scanning mode at 25 °C. 50 μM Fe^{3+}, Fe^{2+}, Mn^{2+}, Co^{2+}, Cu^{2+}, Ni^{2+}, and Ca^{2+} were added at the *down arrow*, respectively

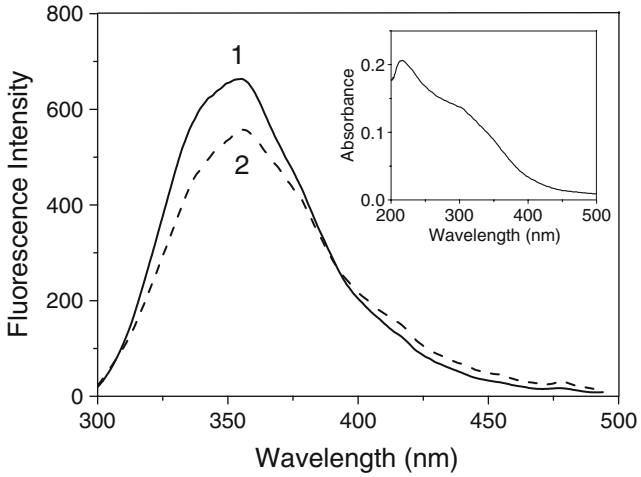

Fig. 2 The effect of Fe^{3+} on the fluorescence of free tryptophan. The fluorescence of 2 μM free tryptophan in 0.05 M Tris–HCl (pH 7.4) was recorded by exciting at 295 nm in the absence of Fe^{3+} (1) and in the presence of 50 μM Fe^{3+} (2), respectively. The *inset figure* depicts the UV absorption spectrum of 50 μM Fe^{3+} in 0.05 M Tris–HCl (pH 7.4)

Trp, which should be the reason for the slight fluorescence quenching of free Trp caused by Fe^{3+}. However, addition of 50 μM $Fe^{3+}$to 1 μM BSA causes a marked fluorescence quenching of the Trp residues in BSA. These results together suggest that Fe^{3+} *ions* have no direct collisional quenching effects on the fluorescence of both the free tryptophan and the Trp *residues* in BSA. Therefore, Fe^{3+} ions-induced fluorescence quenching of BSA is attributed to the complex formation between the protein and Fe^{3+} ions. No Fe^{3+} ions-induced shift in the emission maximum of BSA indicates that the binding of Fe^{3+} to BSA does not markedly *perturb* the microenvironment around the tryptophan residues. Therefore Fe^{3+} ions probably do not bind directly to Trp residues in BSA.

Equilibrium dialysis

Equilibrium dialysis was performed to examine whether BSA binds with Fe^{3+}. According to Eq. 3, the moles of bound Fe^{3+} ions/mol of BSA (r) were calculated to be 0.79±0.01 and 0.98±0.02 (mean ± SE, n=3) at pH 7.4 in the presence of 50 μM Fe^{3+} and 100 μM Fe^{3+}, respectively. This result further confirms that BSA indeed binds with Fe^{3+} and each BSA molecule has one Fe^{3+}-binding site.

Fluorescence titration

The fluorescence titration of BSA with Fe^{3+} was performed to determine the dissociation constant (K_d) of between BSA and Fe^{3+}. Figure 3 shows the fluorescence titration of BSA with Fe^{3+} at different temperatures. Both titration curves could be best fitted to a simple bimolecular equilibrium binding model (Eq. 1). The goodness of the fit of a simple bimolecular equilibrium binding model indicates that haem-free BSA possesses only one specific Fe^{3+}-binding site. The average apparent K_d values for the interaction of Fe^{3+} and BSA are $3.46\times10^{-8}\pm3\times10^{-10}$ M at 37 °C and $3.30\times10^{-8}\pm5\times10^{-10}$ M at 25 °C, respectively. Collisional quenching depends upon diffusion. Since higher temperature results in larger diffusion coefficients, the bimolecular dissociation constant is expected to decrease with increasing temperature. In contrast, increased temperature is likely to result in decreased stability of the complex of fluorophore and quencher, and thus higher value of dissociation constant between fluorophore and quencher [39]. The increase of K_d value for the interaction of Fe^{3+} and BSA with increasing temperature further demonstrates that the Fe^{3+}-induced fluorescence quenching is not due to collisional quenching of BSA by Fe^{3+}, but the nonfluorescent complex formation between BSA and Fe^{3+}.

UV and fourth-derivative spectroscopy

Protein ultraviolet absorption spectra at around 280 nm are known to sensitive to the polarity for the surrounding environments of three amino acid residues (Tyr, Trp and Phe) which contribute to protein UV absorption spectra from 240 to 310 nm. In order to study the Fe^{3+}-induced microenvironment change of BSA, the UV absorption and fourth-derivative spectrum of BSA have been measured. Figure 4a shows the UV absorption spectra of BSA and Fe^{3+}-BSA. UV absorption of BSA at around 253 nm slightly increases upon the binding

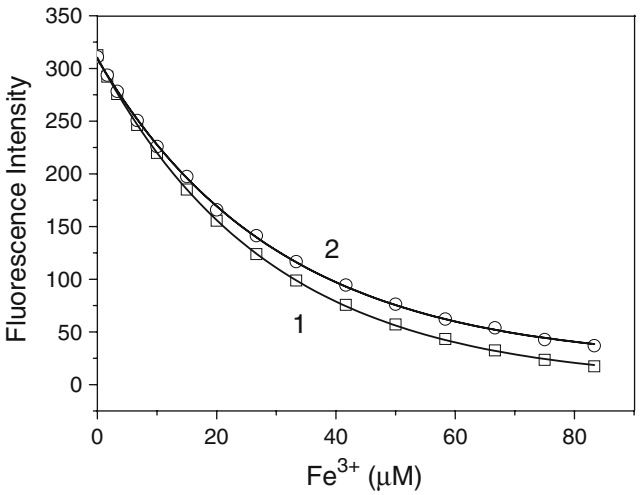

Fig. 3 The fluorescence titration of BSA with Fe^{3+}. One micromolar concentration of BSA in 0.05 M Tris–HCl (pH 7.4) was titrated with the Fe^{3+} at 37 °C (1) and at 25 °C (2), respectively. The solution of Fe^{3+} at an appropriate concentration was added to 1 ml of 1 μM BSA in 0.05 M Tris–HCl (pH 7.4) serially in small aliquots, and the fluorescence intensities at 348 nm were recorded after each titration with excitation at 295 nm. The fluorescence intensities were corrected for changes in volume. Solid line represents fit of the data to a bimolecular association model as described in "Materials and methods"

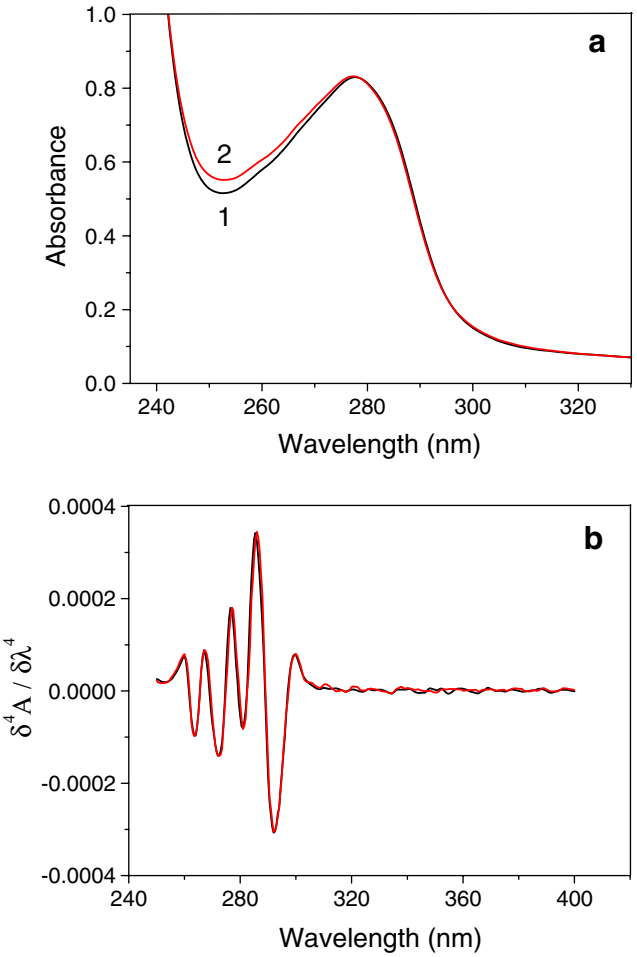

Fig. 4 Absorption (**a**) and fourth-derivative (**b**) spectra of BSA in the absence of Fe^{3+} (*black*) and in the presence of 50 μM Fe^{3+} (*red*). The concentration of BSA is 1.2 mg/ml in 0.05 M Tris–HCl, pH 7.4 and an optical path is 1 cm. Scans were performed at 100 nm/min with a fourth-derivative interval of 10 nm

of BSA with Fe^{3+}. As shown in Fig. 4b, both BSA and Fe^{3+}-BSA have a very similar fourth-derivative spectrum. The result suggests that the interaction between BSA and Fe^{3+} does not induce obvious changes of the environments of Tyr, Trp and Phe residues in BSA, which further demonstrates that Fe^{3+} ions do not bind with Trp residues in BSA.

Circular dichroism (CD) spectra

CD measurements were carried out to study the effects of Fe^{2+} and Fe^{3+} on the secondary structure of BSA. As shown in Fig. 5, no obvious changes have been observed for the CD spectrum of BSA after addition of 50 μM Fe^{2+} or Fe^{3+}, suggesting that both Fe^{2+} and Fe^{3+} have no effects on the secondary structure of BSA. This result indicates that Fe^{2+} ions do not induce a conformational transition of BSA. Therefore, the hysteretic effect of Fe^{2+} on the fluorescence of BSA is probably caused by the possible oxidation of Fe^{2+} to Fe^{3+}.

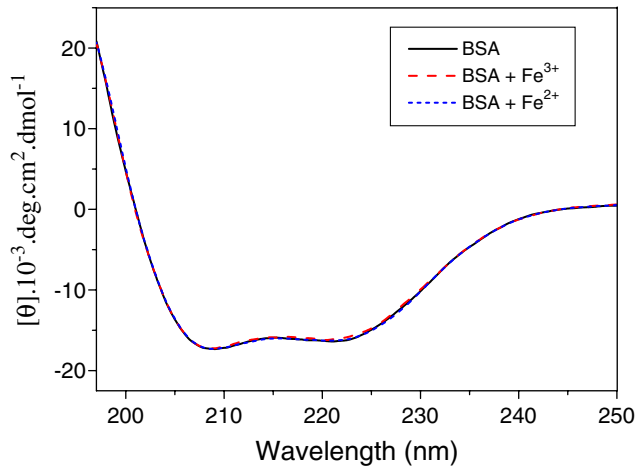

Fig. 5 The effects of Fe^{3+} and Fe^{2+} ions on the CD of BSA. The concentration of BSA is 0.15 mg/ml in 0.05 M Tris–HCl buffer (pH 7.4) in the absence of iron ion (*solid line*) and in the presence of 50 μM Fe^{3+} (*dash line*) and 50 μM Fe^{2+} (*short dash line*)

Oxygen-dependent oxidation of Fe^{2+} to Fe^{3+}

To determine whether the oxygen in the solution is associated with the time-dependent fluorescence quenching of BSA by Fe^{2+}, we deoxygenated the solution of 1 μM BSA in 0.05 M Tris–HCl (pH 7.4) and the solution of Fe^{2+} by flushing with argon before the spectrum was recorded. As shown in Fig. 6 (curve 1), a slow time-dependent fluorescence quenching of BSA by 50 μM Fe^{2+} was observed when the sample solution was deoxygenated by flushing with argon for 5 min before the spectrum was recorded. The kinetics of Fe^{2+}-induced fluorescence

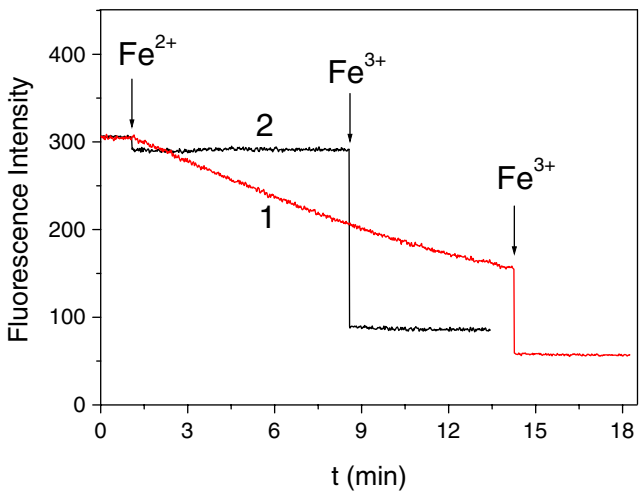

Fig. 6 The effect of oxygen on the time-dependent fluorescence quenching of BSA by Fe^{2+}. The solution of 1 μM BSA in 0.05 M Tris–HCl (pH 7.4) and the solutions of Fe^{2+} and Fe^{3+} were deoxygenated by flushing with argon for 5 min (1) and 20 min (2) before the spectrum was recorded. 50 μM Fe^{2+} and Fe^{3+} were added at the *down arrow*, respectively. The fluorescence of BSA was measured at 348 nm by exciting at 295 nm in time-scanning mode at 25 °C

quenching was also best fitted to a one-exponential term yielding quenching rate constant value of 0.056± 0.001 min^{-1}. The quenching rate constant value decreases from 0.131±0.001 min^{-1} to 0.056±0.001 min^{-1} after part deoxygenization of the sample solution. As shown in Fig. 6 (curve 2), no hysteretic effect of Fe^{2+} on the fluorescence of BSA was observed when the sample solution was extensively deoxygenated by flushing with argon for 20 min before the spectrum was recorded. This result indicates that Fe^{2+} ions can not induce time-dependent fluorescence quenching of BSA after complete deoxygenization of the sample solution. Figure 6 also shows that addition of 50 μM Fe^{3+} ions to the reaction mixture of 1 μM BSA and 50 μM Fe^{2+} ions further results in a marked quenching of the fluorescence of BSA either for curve 1 or for curve 2. These results demonstrate that the time-dependent fluorescence quenching of BSA by Fe^{2+} is not due to the Fe^{2+}-induced conformational change of BSA, but the oxygen-dependent oxidation of Fe^{2+} to Fe^{3+}.

Figure 7a shows the effect of the concentration of Fe^{2+} on the time-dependent fluorescence quenching of BSA by Fe^{2+}. The Fe^{2+}-induced fluorescence quenching of BSA **is** accelerated by the increase of the concentration of Fe^{2+}. Interestingly, a plot of the quenching rate constant value of Fe^{2+} against the concentration of Fe^{2+} gives a straight line (Fig. 7b). This linear relationship between the quenching rate constant value of Fe^{2+} and the concentration of Fe^{2+} shows that there is a second-order process in Fe^{2+}-induced fluorescence quenching of BSA.

To determine the behaviors of the oxidization of Fe^{2+} by the oxygen in solution in the absence of BSA, 50 μM Fe^{2+} solution containing 0.05 M Tris–HCl (pH 7.4) was prepared from stock solution of Fe^{2+} and opened to air for different time at 25 °C before addition of 1 μM BSA. The fluorescence of the reaction mixture was measured immediately after addition of 1 μM BSA to 50 μM Fe^{2+}. Figure 8a shows the effect of the incubation time of 50 μM Fe^{2+} with the oxygen dissolved in 0.05 M Tris–HCl (pH 7.4) solution in the absence of BSA under aerobic conditions on the time-dependent fluorescence quenching of BSA by Fe^{2+}. The fluorescence intensity of BSA at 0 min for each curve in Fig. 8a decreases with the increase of the incubation time of 50 μM Fe^{2+} with the oxygen dissolved in 0.05 M Tris–HCl (pH 7.4) solution in the absence of BSA under aerobic conditions, suggesting that Fe^{2+} is also oxidized by the oxygen in solution in the absence of BSA. Figure 8b shows the effect of the incubation time of 50 μM Fe^{2+} with the oxygen dissolved in 0.05 M Tris–HCl (pH 7.4) solution opened to air in the absence of BSA on the fluorescence intensity of BSA at 0 min for each curve in Fig. 8a. The kinetics of the fluorescence quenching was also best fitted to a one-exponential term yielding quenching rate constant value of

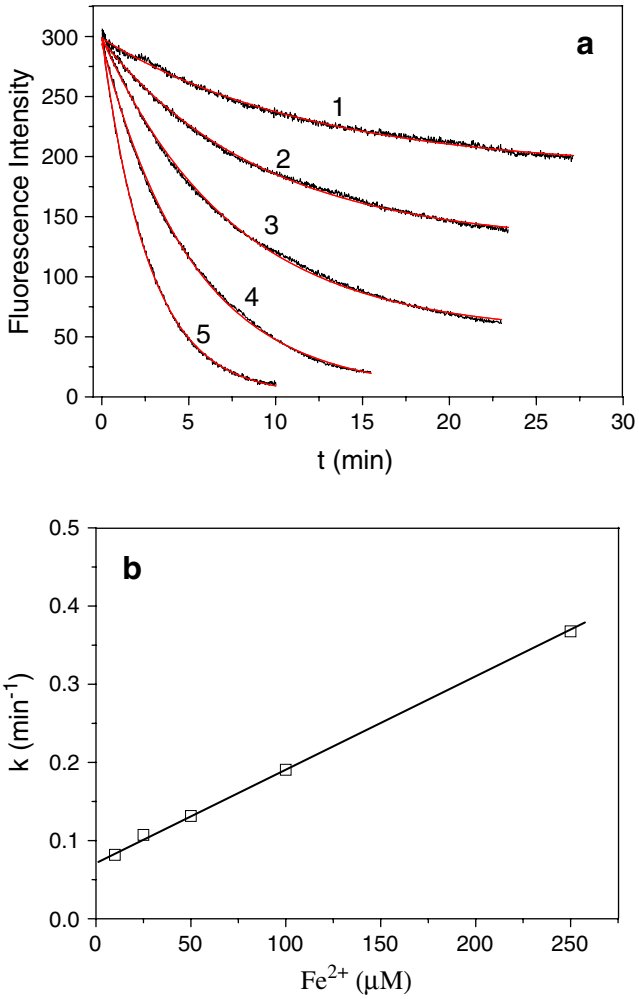

Fig. 7 The effect of the concentration of Fe^{2+} on the time-dependent fluorescence quenching of BSA by Fe^{2+}. **a** The fluorescence of 1 μM BSA in 0.05 M Tris–HCl (pH 7.4) in the presence of 10 (1), 25 (2), 50 (3), 100 (4) and 250 μM Fe^{2+} (5) was measured at 348 nm by exciting at 295 nm in time-scanning mode at 25 °C, respectively. The data were fit to a single-exponential decay model. **b** The effect of the concentration of Fe^{2+} on the oxidation rate constant of Fe^{2+}

0.113±0.002 min^{-1}. Because the oxygen in solution slowly oxidized Fe^{2+} to Fe^{3+} and the produced Fe^{3+} fast bound to BSA and resulted in the fluorescence quenching of BSA, the decrease rate of the fluorescence intensity of BSA at 0 min for each curve in Fig. 8a should be equal to the oxidation rate of Fe^{2+} by the oxygen dissolved in solution in the absence of BSA, namely, the oxidation rate of Fe^{2+} by oxygen in the absence of BSA was equal to 0.113± 0.002 min^{-1}, which was less than that in the presence of 1 μM BSA.

Discussion

The present study aims to investigate whether haem-free BSA binds with ironic ions and if the interaction causes a

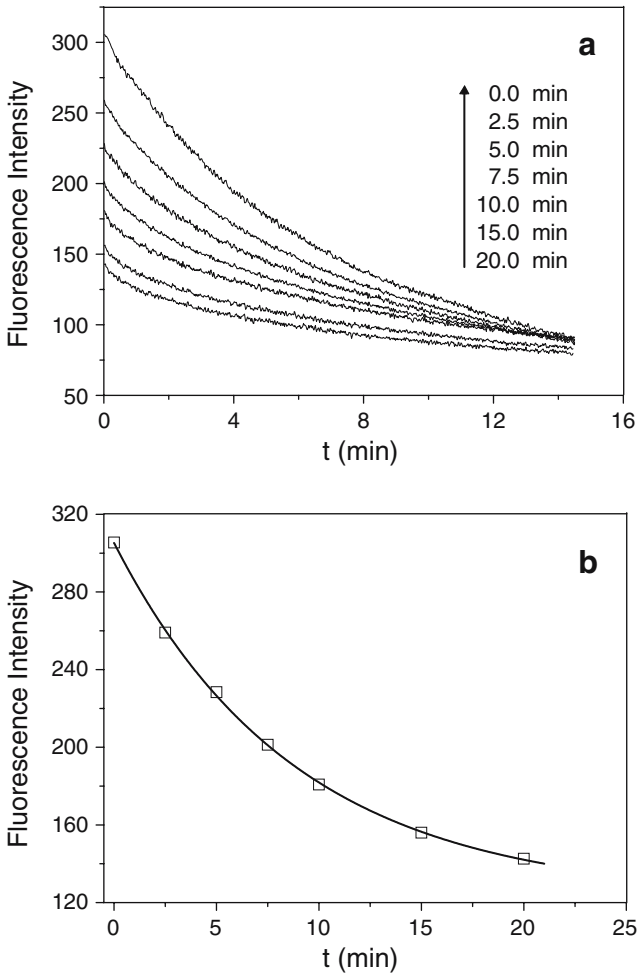

Fig. 8 The effect of the incubation time of 50 μM Fe^{2+} with the oxygen dissolved in 0.05 M Tris–HCl (pH 7.4) solution in the absence of BSA under aerobic conditions on the time-dependent fluorescence quenching of BSA by Fe^{2+}. **a** 2 ml of 50 μM Fe^{2+} was made by diluting stock solution of Fe^{2+} into the buffer solution. The sample was opened to air at 25 °C for 0, 2.5, 5, 7.5, 10, 15 and 20 min before the spectrum was recorded. The spectrum was recorded after addition of 1 μM BSA at 348 nm by exciting at 295 nm in time-scanning mode at 25 °C. **b** The effect of the incubation time of 50 μM Fe^{2+} with the oxygen dissolved in 0.05 M Tris–HCl (pH 7.4) solution in the absence of BSA under aerobic conditions on the fluorescence intensity of BSA at the beginning of each recordation. The data were fit to a single-exponential decay model

slow conformational transition of BSA. The above results reveal that haem-free BSA binds with one Fe^{3+} ion. Figure 1 shows that Fe^{3+} binds fast to BSA and this binding does not cause any hysteretic effect on BSA detected by fluorescence. No obvious effects on the fourth-derivative spectrum and CD spectrum of BSA have been observed upon the binding of Fe^{3+} to BSA, suggesting that Fe^{3+} ions have no obvious effects on the secondary structure of BSA and that Fe^{3+} ions do not bind with Trp residues in BSA. However, the interaction between Fe^{3+} and BSA results in the significant fluorescence quenching of BSA (Fig. 1). As shown in Fig. 2, Fe^{3+} ions have no direct collisional quenching effects on the fluorescence of free tryptophan. Therefore, the Fe^{3+}-induced fluorescence quenching of BSA is caused by the nonfluorescent complex formation between BSA and Fe^{3+}, which is further confirmed by the fact that the K_d value for the interaction of Fe^{3+} and BSA increases with increasing temperature. Because the emission spectrum of BSA overlaps with the absorption of Fe^{3+} (Fig. 2), the fluorescence energy transfer from the Trp residues in BSA to the bound Fe^{3+} occurs. Fe^{3+} absorbs photons and returns to the ground state without emission of a photon. Fe^{3+}-induced fluorescence quenching of BSA occurs as a result of the formation of a nonfluorescent ground state complex between BSA and Fe^{3+}. The efficiency of energy transfer is limited only by the distance of closest possible approach between donor and acceptor [39]. The Fe^{3+}-induced marked fluorescence quenching of BSA indicates that the Fe^{3+}-binding site is adjacent to both Trp residues in BSA. The fluorescence of 1 μM Fe^{3+}-BSA at 348 nm obviously increases after addition of 10 mM EDTA (data not shown), suggesting that the binding of Fe^{3+} to BSA is reversible

It has been reported that the interaction of BSA with Co^{2+} or Ni^{2+} has a subsequent effect on BSA as determined by UV spectra [25, 34]. However, these hysteretic effects for the interaction between BSA and Co^{2+} or Ni^{2+} are undetectable by fluorescence spectra. Co^{2+} or Ni^{2+}-induced slow conformational change of BSA should not affect the fluorescence of its Trp residues. Interestingly, a notable hysteretic effect on the fluorescence of BSA has been observed after addition of 50 μM Fe^{2+} to BSA solution under aerobic conditions. The hysteretic effect of Fe^{2+} on the fluorescence of BSA was completely inhibited under anaerobic conditions. Addition of 50 μM Fe^{2+} to BSA solution does not cause *any change for the secondary structure* of BSA as indicated by CD spectra (Fig. 5). All these observations taken together suggest that the hysteretic effect of Fe^{2+} on fluorescence of BSA is not caused by the Fe^{2+}-induced conformational change of BSA, but the oxygen-dependent oxidation of Fe^{2+} to Fe^{3+}.

It has been reported that under aerobic conditions, superoxide (O_2^-), hydroxyl radical ($^{\cdot}OH$), and hydrogen peroxide (H_2O_2) are produced in aqueous solutions of ferrous salts by the reaction [40]:

$$Fe^{2+} + O_2 \rightarrow Fe^{3+} + O_2^- \quad (4)$$

$$2O_2^- + 2H^+ \rightarrow H_2O_2 + O_2 \quad (5)$$

$$Fe^{2+} + H_2O_2 \rightarrow HO^{\cdot} + HO^- + Fe^{3+} \quad (6)$$

Because Fe^{3+} ions are the products for the Reactions 4 and 6, the binding between BSA and Fe^{3+} decreases the

concentration of Fe^{3+} and therefore increases the rates of both Reactions 4 and 6, which may be the reason why BSA can accelerate the oxygen-dependent oxidation of Fe^{2+} to Fe^{3+}. Since the oxidation of Fe^{2+} to Fe^{3+} dependents on O_2, the oxidation of Fe^{2+} to Fe^{3+} is inhabited under anaerobic conditions, as a result, no hysteretic effect of Fe^{2+} on the fluorescence of BSA has been observed under anaerobic conditions (Fig. 6).

Albumin represents 52–60% of the total plasma protein and plays an important role in the transport and storage of hormones, fatty acids and drugs, acting by regulating their plasma concentrations [41]. In particular, its role in the transport of essential metal ions has received considerable attention. Transferrin, which composes about 7–10% of plasma protein, is a non-heme iron binding glycoprotein [42]. Fe^{3+} ions are transported in plasma mainly by transferring [43]. Both Fe^{2+} and Fe^{3+} ions bind to haem-serum albumin through the haem-iron complex [29]. The above results indicate that Fe^{3+} also bind to haem-free BSA. Therefore BSA may take part in non-transferrin bound iron transfer.

Buss et al. [44] reported that the addition of BSA to the extracellular medium increased the extent of iron release in a concentration-dependent manner. BSA-induced iron release was presumably explained by the binding between BSA and the iron-chelator complexes. The binding of BSA with Fe^{3+} may be another reason for the BSA-induced iron release.

Iron has many uses in biological systems because of its excellent catalytic versatility. However, the chemical properties of iron that allow this versatility are also responsible for its potential toxicity. Iron in excess, due to its catalysis of one-electron redox chemistry, plays a key role in the formation of oxygen radicals, which cause oxidative damage to cellular structures [44]. For example, excess hepatic iron may be both directly and indirectly hepatocarcinogenic [45]. Iron overload, may tip the immunoregulatory balance unfavorably to allow increased growth rates of cancer cells and infectious organisms [46]. Because of the limited ability of the body to excrete excess iron, iron overload usually develops in transfusion-dependent patients, such as those with β-thalassemia, aplastic anemia, or myelodysplastic syndrome. Iron-mediated toxicity has been ascribed to Fe(II), which reacts with oxygen to generate free radicals that damage macromolecules and cause cell death. Typically, no free Fe^{2+} is present because all iron is bound to transferrin in a redox-inactive Fe^{3+} form. The serum albumins are more abundant protein in blood serum than transferrin. *BSA is expected to provide a temporary sink for excess iron, due to its affinity for* Fe^{3+}. *The above observation raises a new question whether BSA protects blood against the toxic effects of excess free iron. Further investigation is necessary to clarify this issue.*

In summary, haem-free BSA possesses one specific Fe^{3+}-binding site. The binding of Fe^{3+} to BSA neither causes any hysteretic effect on the fluorescence of BSA, nor influences the secondary structure of BSA. Addition of 50 μM Fe^{2+} ions to 1 μM BSA results in an obvious hysteretic effect on the fluorescence of BSA. The time-dependent fluorescence quenching of BSA by Fe^{2+} is not caused by the Fe^{2+}-induced conformational change of BSA, but the oxygen-dependent oxidation of Fe^{2+} to Fe^{3+}. Fe^{2+} undergoes an oxygen-dependent oxidation to Fe^{3+} under aerobic conditions, which is accelerated by the interaction of BSA with Fe^{3+} and extensively inhibited under anaerobic conditions. The results suggest that BSA may take part in non-transferrin bound iron transfer.

Acknowledgment This research was supported by grants from the National Natural Science Foundation of China (Grant No. 20571069, 20171041, X. L. Xu).

References

1. Petrat F, Paluch S, Dogruoz E, Dorfler P, Kirsch M, Korth HG, Sustmann R, de Groot H (2003) Reduction of Fe(III) ions complexed to physiological ligands by lipoyl dehydrogenase and other flavoenzymes in vitro: implications for an enzymatic reduction of Fe(III) ions of the labile iron pool. J Biol Chem 278:46403–46413
2. Beaumont C (2004) Molecular mechanisms of iron homeostasis. Med Sci (Paris) 20:68–72
3. Zhao G, Arosio P, Chasteen ND (2006) Iron(II) and hydrogen peroxide detoxification by human H-chain ferritin. An EPR spin-trapping study. Biochemistry 45:3429–3436
4. Bou-Abdallah F, Zhao G, Mayne HR, Arosio P, Chasteen ND (2005) Origin of the unusual kinetics of iron deposition in human H-chain ferritin. J Am Chem Soc 127:3885–3893
5. Ollinger OK, Roberg K (1997) Nutrient deprivation of cultured rat hepatocytes increases the desferrioxamine-available iron pool and augments the sensitivity to hydrogen peroxide. J Biol Chem 272:23707–23711
6. Bou-Abdallah F, Zhao G, Mayne HR, Arosio P, Chasteen ND (2005) Origin of the unusual kinetics of iron deposition in human H-chain ferritin. J Am Chem Soc 127(11):3885–3893
7. Kakhlon O, Cabantchik ZI (2002) The labile iron pool: characterization, measurement, and participation in cellular processes(1). Free Radic Biol Med 33:1037–1046
8. Banerjee T, Singh SK, Kishore N (2006) Binding of naproxen and amitriptyline to bovine serum albumin: biophysical aspects. J Phys Chem B 110:24147–24156
9. Hamilton JA, Era S, Bhamidipati SP, Reed RG (1991) Locations of the three primary binding sites for long-chain fatty acids on bovine serum albumin. Proc Natl Acad Sci USA 88:2051–2054
10. Curry S, Mandelkow H, Brick P, Franks N (1998) Crystal structure of human serum albumin complexed with fatty acid reveals an asymmetric distribution of binding sites. Nat Struct Biol 5:827–835
11. Petitpas I, Petersen CE, Ha CE, Bhattacharya AA, Zunszain PA, Ghuman J, Bhagavan NV, Curry S (2003) Structural basis of albumin–thyroxine interactions and familial dysalbuminemic hyperthyroxinemia. Proc Natl Acad Sci USA 100:6440–6445

12. Zunszain PA, Ghuman J, Komatsu T, Tsuchida E, Curry S (2003) Crystal structural analysis of human serum albumin complexed with hemin and fatty acid. BMC Struct Biol 7:3–6
13. Ghuman J, Zunszain PA, Petitpas I, Bhattacharya AA, Otagiri M, Curry S (2005) Structural basis of the drug-binding specificity of human serum albumin. J Mol Biol 353:38–52
14. Curry S, Mandelkow H, Brick P, Franks N (1998) Crystal structure of human serum albumin complexed with fatty acid reveals an asymmetric distribution of binding sites. Nat Struct Biol 5:827–835
15. Bhattacharya AA, Curry S, Franks NP (2000) Binding of the general anesthetics propofol and halothane to human serum albumin: high-resolution crystal structures. J Biol Chem 275:38731–38738
16. Petitpas I, Bhattacharya AA, Twine S, East M, Curry S (2001) Crystal structure analysis of warfarin binding to human serum albumin: anatomy of drug site I. J Biol Chem 276:22804–22809
17. Karnaukhova E (2007) Interactions of human serum albumin with retinoic acid, retinal and retinyl acetate. Biochem Pharmacol 73:901–910
18. Qu SS, Liu Y, Wang TZ, Gao WY (2002) Thermodynamics of binding of cadmium to bovine serum albumin. Chemosphere 46:1211–1214
19. Sadler PJ, Viles JH (1996) ^{1}H and ^{113}Cd NMR investigations of Cd^{2+} and Zn^{2+} binding sites on serum albumin: competition with Ca^{2+}, Ni^{2+}, Cu^{2+}, and Zn^{2+}. Inorg Chem 35:4490–4496
20. Masuoka J, Saltman P (1994) Zinc (II) and copper (II) binding to serum albumin. J Biol Chem 269:25557–25561
21. Masuoka J, Hegenaurer J, Van Dyke BR, Saltman P (1993) Intrinsic stoichiometric equilibrium constants for the binding of zinc(II) and copper(II) to the high affinity site of serum albumin. J Biol Chem 268:21533–21537
22. Ohyoshi E, Hamada Y, Nakata K, Kohata S (1999) The interaction between human and bovine serum albumin and zinc studied by a competitive spectrophotometry. J Inorg Biochem 75:213–218
23. Zhang Y, Wilcox DE (2002) Thermodynamic and spectroscopic study of Cu(II) and Ni(II) binding to bovine serum albumin. J Biol Inorg Chem 7:327–337
24. Mothes E, Faller P (2007) Evidence that the principal Co(II)-binding site in human serum albumin is not at the N-terminus: implication on the albumin cobalt binding test for detecting myocardial ischemia. Biochemistry 46:2267–2274
25. Liang H, Huang J, Tu CQ, Zhang M, Zhou YQ, Shen PW (2001) The subsequent effect of interaction between Co^{2+} and human serum albumin or bovine serum albumin. J Inorg Biochem 85:167–171
26. Zhong K, Xia J, Wei W, Hu Y, Tao H, Liu W (2005) A kinetic model and its parameter estimation for the process of binding copper to human serum albumin by a voltammetric method. Anal Bioanal Chem 381:1552–1557
27. Qu SS, Liu Y, Wang TZ, Gao WY (2002) Thermodynamics of binding of cadmium to bovine serum albumin. Chemosphere 46:1211–1214
28. Ayranci E, Duman O (2004) Binding of lead ion to bovine serum albumin studied by ion selective electrode. Protein Pept Lett 11:331–337
29. Baroni S, Mattu M, Vannini A, Cipollone R, Aime S, Ascenzi P, Fasano M (2001) Effect of ibuprofen and warfarin on the allosteric properties of haem-human serum albumin. A spectroscopic study. Eur J Biochem 268:6214–6220
30. Fasano M, Baroni S, Vannini A, Ascenzi P, Aime S (2001) Relaxometric characterization of human hemalbumin. J Biol Inorg Chem 6:650–658
31. Huang YB, Komatsu T, Wang RM, Nakagowa A, Tsuchida E (2006) Poly(ethylene glycol)-conjugated human serum albumin including iron porphyrins: surface modification improves the O-2-transporting ability. Bioconjug Chem 17:393–398
32. Ogino T, Okada S (1995) Oxidative damage of bovine serum albumin and other enzyme proteins by iron–chelate complexes. Biochim Biophys Acta 1245:359–365
33. Buss JL, Arduini E, Ponka P (2002) Mobilization of intracellular iron by analogs of pyridoxal isonicotinoyl hydrazone (PIH) is determined by the membrane permeability of the iron–chelator complexes. Biochem Pharmacol 64:1689–1701
34. Liang H, Ouyang D, Hu XY, Tai JZ, He JT, Zhou YQ (1998) Structural studies on metal-serum albumin III. Slow conformational transition of HAS and BSA induced by Ni^{2+} ion. Acta Chimica Sinica 56:662–667
35. Xu XL, Chen JX, Zhang LY, Wang SY, Shen DK, Liu QL (2007) Calcium ion-induced stabilization and refolding of agkisacutacin from *Agkistrodon acutus* venom studied by fluorescent spectroscopy. J Fluoresc 17:215–221
36. Mojzisova H, Bonneau S, Vever-Bizet C, Brault D (2007) The pH-dependent distribution of the photosensitizer chlorin e6 among plasma proteins and membranes: a physico-chemical approach. Biochim Biophys Acta 1768:366–374
37. Maji SK, Amsden JJ, Rothschild KJ, Condron MM, Teplow DB (2005) Conformational dynamics of amyloid β-protein assembly probed using intrinsic fluorescence. Biochemistry 44:13365–13376
38. Leonard DA, Satoskar RS, Wu WJ, Bagrodia S, Cerione RA, Manor D (1997) Use of a fluorescence spectroscopic readout to characterize the interactions of Cdc42Hs with its target/effector, mPAK-3. Biochemistry 36:1173–1180
39. Lakowicz JR (1983) Principles of fluorescence spectroscopy. Plenum, New York
40. Grady JK, Chen Y, Chasteen ND, Harris DC (1989) Hydroxyl radical production during oxidative deposition of iron in ferritin. J Biol Chem 264:20224–20229
41. Sugio S, Kashima A, Mochizuki S, Noda M, Kobayashi K (1999) Crystal structure of human serum albumin at 2.5 Å resolution. Protein Eng 12:439–446
42. Choi I, Sung K, Kim Y, Parx Y (2004) Effect of transferring on enhancing bioavailability of iron. Biosci Biotechnol Biochem 68:578–583
43. Suyama S, Abe S, Inoue Y, Toukairin A, Ohtake Y, Ohyubo Y (2006) The involvement of transferrin in the uptake of iron-59 by hepatocytes of carbon tetrachloride-damaged rats. Biol Pharm Bull 29:1387–1390
44. Buss JL, Arduini E, Ponka P (2002) Mobilization of intracellular iron by analogs of pyridoxal isonicotinoyl hydrazone (PIH) is determined by the membrane permeability of the iron–chelator complexes. Biochem Pharmacol 64:1689–1701
45. Asare GA, Mossanda KS, Kew MC, Paterson AC, Kahler-Venter CP, Siziba K (2006) Hepatocellular carcinoma caused by iron overload: a possible mechanism of direct hepatocarcinogenicity. Toxicology 219:41–52
46. Walker EM Jr, Walker SM (2000) Effects of iron overload on the immune system. Ann Clin Lab Sci 30:354–365